Liquid Crystals
Publication details, including instructions for authors and subscription information:
http://www.informaworld.com/smpp/title~content=t713926090

Phase diagram of a two-frequency chiral nematic mixture in an electric field

Slavomír Pirkl[a]
[a] University of Chemical Technology, Pardubice, Czech Republic

To cite this Article Pirkl, Slavomír(1994) 'Phase diagram of a two-frequency chiral nematic mixture in an electric field', Liquid Crystals, 16: 6, 973 — 982
To link to this Article: DOI: 10.1080/02678299408027867
URL: http://dx.doi.org/10.1080/02678299408027867

LIQUID CRYSTALS, 1994, VOL. 16, NO. 6, 973–982

Phase diagram of a two-frequency chiral nematic mixture in an electric field

by SLAVOMÍR PIRKL
University of Chemical Technology, 532 10 Pardubice, Czech Republic

(*Received 16 August 1993; accepted 11 September 1993*)

The behaviour of a chiral nematic mixture with low frequency dielectric relaxtion was studied between two electrodes, with homeotropic anchoring, in the presence of an AC electric field E. The phase diagram in the parameter plane $(d/p, E)$ was determined for this mixture which could be dielectrically negative or positive in different frequency ranges. The determination was carried out by changing the sample thickness d and both the amplitude and frequency of the electric field at a constant cholesteric pitch p.

1. Introduction

Two control parameters in electro-optic cells involving cholesteric liquid crystals are the frustration ratio of the cell gap over the quiescent pitch $(d/p = C)$ and the applied voltage V. Recently, specific (V, C)-phase diagrams have been established both experimentally and theoretically for large pitch cholesteric liquid crystals with both positive [1] and negative [2, 3] dielectric anisotropy under homeotropic anchoring conditions. It was shown that in the (V, C) parameter plane, different types of situation could be characterized, such as a homeotropic nematic phase (unwound cholesteric), isolated doubly twisted fingers, a periodic pattern of fingers arranged side by side, and a transient singly twisted translationally invariant configuration (TIC).

It is also well known that the cholesteric structure is fully unwound without an electric field when the distance d between homeotropically orienting surfaces does not exceed a certain critical value $d_c \approx p$ [4, 5, 6]. The dimensionless ratio $C = d/p$ is the control parameter for this unwinding transition.

In this paper, the (V, C)-phase diagram for a cholesteric liquid crystal with low frequency dielectric relaxation in an electro-optic cell with homeotropic boundary conditions is described. In this case, the dielectric anisotropy $\Delta\varepsilon$ is negative and positive for $f > f_0$ and $f < f_0$, respectively, where f_0 is the isotropy (cross-over) frequency at which $\Delta\varepsilon = 0$. Therefore, contrary to previous experiments, both types of (V, C)-phase diagram can be determined in the same cell using a control voltage with sufficiently different frequencies.

2. Experimental part

The two-frequency chiral nematic liquid crystal with an appropriate pitch was prepared by adding the chiral agent ZLI 811 (E. Merck) to the commercial 2F-nematic mixture ZLI 2979 (E. Merck). Basic parameters of the mixture investigated are listed in the table.

The quiescent pitch p of a chiral structure was measured by the conventional Cano-wedge method. The critical sample thickness d_c at which the chiral structure

0267–8292/94 $10·00

Composition and physical properties (manufacturer's data) at 20°C for the mixture investigated.

Basic mixture	ZLI 811 wt%	T_i/°C	Δn	$\Delta\varepsilon_L$	$\Delta\varepsilon_H$	f_0/kHz	p/μm	d_c/μm
ZLI 2979	0·615	126	0·1216	+2·0	−1·2	2·0	16	16·6

T_i, clearing temperature; Δn, birefringence; f_0, isotropy (cross-over) frequency; $\Delta\varepsilon_L$, $\Delta\varepsilon_H$, low and high frequency dielectric anisotropies; respectively; p, cholesteric pitch; d_c, critical thickness.

spontaneously unwinds under homeotropic anchoring conditions was calculated from the measured distance between the cholesteric–nematic boundary and the tip of the wedge cell, which had a known slope between its lecithin treated surfaces [6, 7].

Texture changes under different electric field intensities E were observed using a special electro-optic cell [1] with a continuously variable distance between the parallel electrodes which were coated with a homeotropically orienting silane. The glass plates with electrodes were fixed to two metallic holders coupled together by three differential screws. The thickness variations of the sample (from 0 to 500 μm) were measured using a LVTD-type transducer ATA 101 (Schaevitz) with an accuracy of $\pm 0{\cdot}05\,\mu$m. Observations were performed in the transmission mode between crossed polarizers using a Leitz polarizing microscope equipped with a photocamera, colour CCD Videocamera CL-700 (Panasonic), colour monitor (Sony), video cassette recorder AG-6760 (Panasonic), and videocopy processor UP-811 (Sony). Square wave a.c. voltages of 0·1 and 30 kHz, respectively, were used for measurements over a range of the positive and or negative dielectric anisotropy regimes. All measurements were made at a temperature of 28°C.

In order to establish the phase diagram for the dielectrically positive liquid crystal ($\Delta\varepsilon > 0$), the following procedure was applied: for a given thickness $d > d_c$, the low frequency voltage V ($f = 100$ Hz) was increased until the cholesteric structure completely disappeared and the nematic phase was the only stable phase. Then the voltage was abruptly lowered to a particular value and the newly arising textures or structures were observed. Then the boundary between metastable and fully unstable cholesteric fingers was determined at a slowly increasing voltage.

All observations made for the dielectrically negative liquid crystal ($\Delta\varepsilon < 0$) were carried out at a thickness $d < d_c$, ensuring the stability of the nematic structure without an electric field. Contrary to the preceding procedure, the high frequency voltage ($f = 30$ kHz) was abruptly increased from zero to a required value and the chiral textures that arose were observed. The limit separating regions of unstable and metastable fingers was determined by decreasing the voltage abruptly to a required value.

3. Results and discussion

At the start of the electro-optic measurements, the critical unwinding thickness d_c at zero voltage was measured by slowly decreasing the sample thickness until the homeotropic nematic phase spread throughout the whole sample (see figure 1). Thus determined the value closely corresponds (within 2 per cent) to the value listed in the table. During this procedure, a certain thickness d_x (and the corresponding value $C_x = 1{\cdot}41$) at which black spots (homeotropic texture) first appeared in the striped

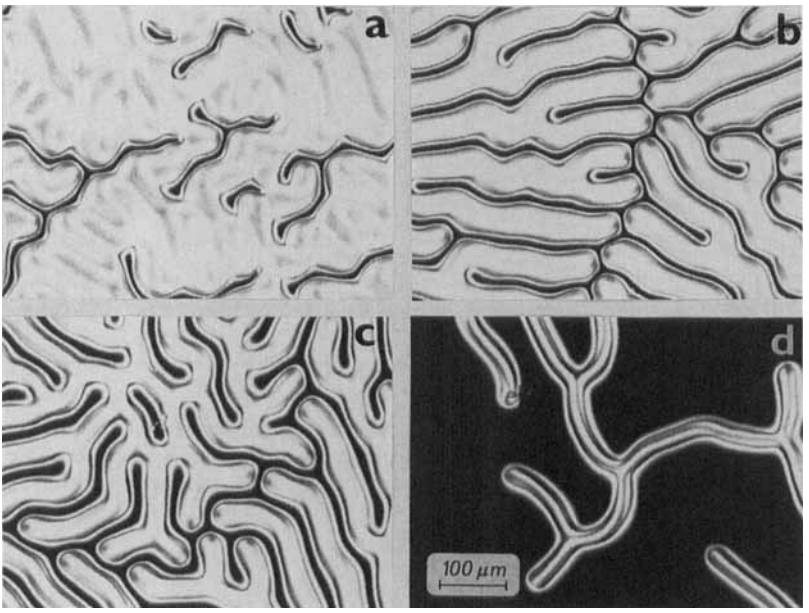

Figure 1. Quiescent periodic texture at different d/p ratios (zero voltage, crossed polarizers): (*a*) $C = 1{\cdot}35$, (*b*) $C = 1{\cdot}29$, (*c*) $C = 1{\cdot}18$, (*d*) $C = 1{\cdot}00$.

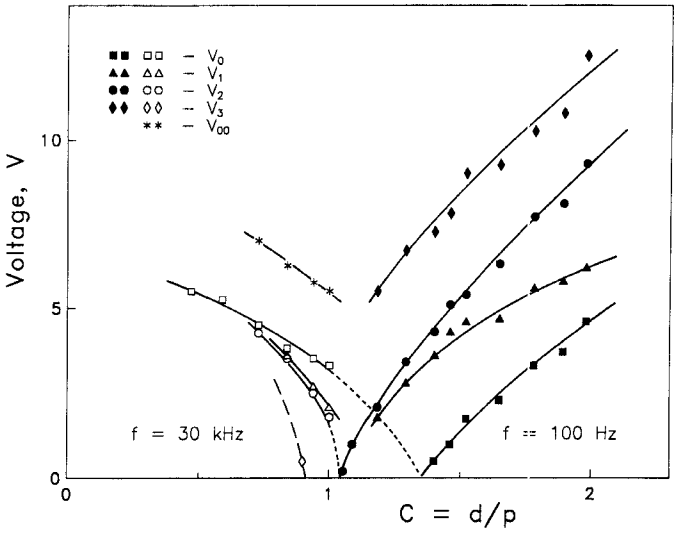

Figure 2. Experimental phase diagram of the 2F-chiral nematic mixture under investigation at 28°C. Voltage frequency $f = 30$ kHz (open symbols) and $f = 100$ Hz (full symbols). For explanation, see also the text and the legend of figure 3.

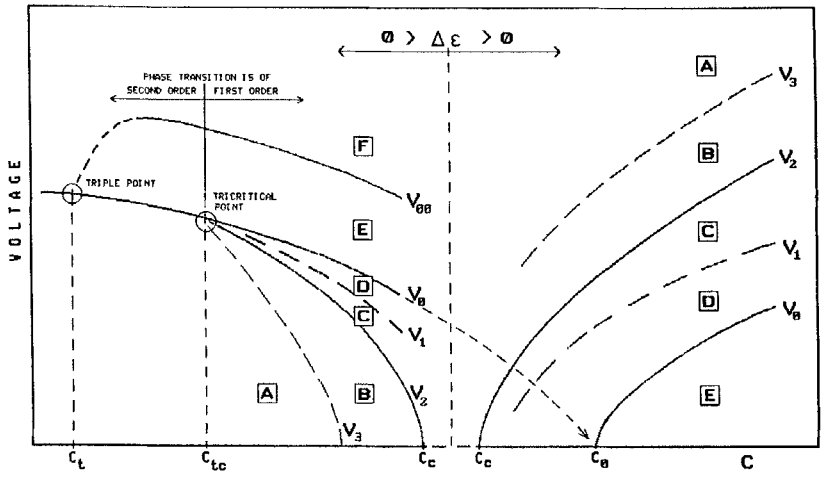

Figure 3. Schematic phase diagram of the dielectrically negative and positive cholesteric mesophase in an electric field. *A*, homeotropic nematic phase; *B*, metastable isolated fingers; *C*, growing isolated fingers; *D*, growing periodic patterns—splitting fingers; *E*, stable periodic patterns; *F*; planar cholesteric texture (TIC). (Reason for the V_i lines, see text.)

cholesteric texture was also observed. This value C_x is in good agreement with C_0 at which $V_0 = 0$ holds (see figure 2 and 3) and also with the value $C_x^* = 1{\cdot}36$ at which bands of homeotropic nematic phase between fingers disappear in the wedge cell [7].

The experimentally established phase diagram is presented in figure 2. Five and six different regions can be distinguished according to the values of C and V for the low ($\Delta\varepsilon > 0$) and the high frequency voltage ($\Delta\varepsilon < 0$), respectively. A number of these regions depend on the value of C. In agreement with previous observations and theoretical considerations [1, 2], the separate regions (for a better understanding see figure 3) correspond to the following solutions:

Region *A*—stable homeotropic nematic phase (N) which is uniformly dark between crossed polarizers. The cholesteric mesophase (Ch) is unstable—fingers break up spontaneously in numerous places.

Region *B*—stable homeotropic N and metastable Ch. The cholesteric fingers disappear gradually from their ends without changes in width. Experimental studies of this region with the high frequency voltage ($f = 30\,\text{kHz}$) were impossible.

Region *C*—stable Ch and metastable N. The isolated fingers are growing only from their two ends (see figure 4). They usually nucleate on dust particles present in the sample, showing that the fingerprint formation is indeed the first order transition. Some rules for finger growth are discussed later.

Region *D*—splitting cholesteric fingers (see figure 5) which grow and fill up the whole space as a periodic fingerprint-like texture. The finger splitting is the requisite condition for achieving a constant mean wavelength in forming domains with a circular geometry. Growth velocity increases as the voltage changes from the value V_1 to the value V_0 (see figure 6) and with increasing d/p ratio.

Region *E*—stable periodic pattern (fingerprint-like texture) which develops from the transiently existing, translationally invariant configuration (TIC) [1] in the whole sample (see figure 7) after an abrupt voltage change from ranges *A* or *B* into range *E*. Near the line V_0, the fingers are separated by homeotropic regions which progressively disappear when the voltage increases (at $f = 30$ kHz) or decreases (at $f = 100$ Hz). In the dielectrically negative phase ($f = 30$ kHz), the stripes 'dissolves' at higher voltages and the planar chiral texture arises.

Region *F*—stable planar chiral nematic texture (or TIC) with the optic axis normal to the electrodes.

The same rules for finger growth were determined as in [1, 2, 3]:

(1) Two types of tip, i.e. a rounded 'normal tip' $\langle + \rangle$ and a sharper 'abnormal' tip $\langle - \rangle$ (see figures 4 and 8), can be experimentally distinguished.
(2) Two different finger configurations are possible: either the two ends of the fingers are identical (both being the normal tips $\langle + + \rangle$) and there is always a defect inside the finger (see figure 8 (A) or there is no defect and the two ends have tips of opposite sign (see figures 4 and 8 (B)).
(3) Only fingers with the normal tip split, while the abnormal tips remain unchanged during the growth (see figure 8 (B)).
(4) Only tips of opposite sign collapse together (see figure 9 (C)), while two tips of the same repel each other and remain separated by a nematic slice (see figure 9 (A)).
(5) Only the abnormal tip can collapse into the side of a finger and form a T-like side branch, while the normal tip is repelled (see figure 9 (B)).
(6) Growth velocity is zero on the line V_2 dividing regions *C* and *B* or *A*, and increases on changing the voltage from the value V_2 to the value V_1 (see figure 6) and with increasing d/p ratio (see figure 10).

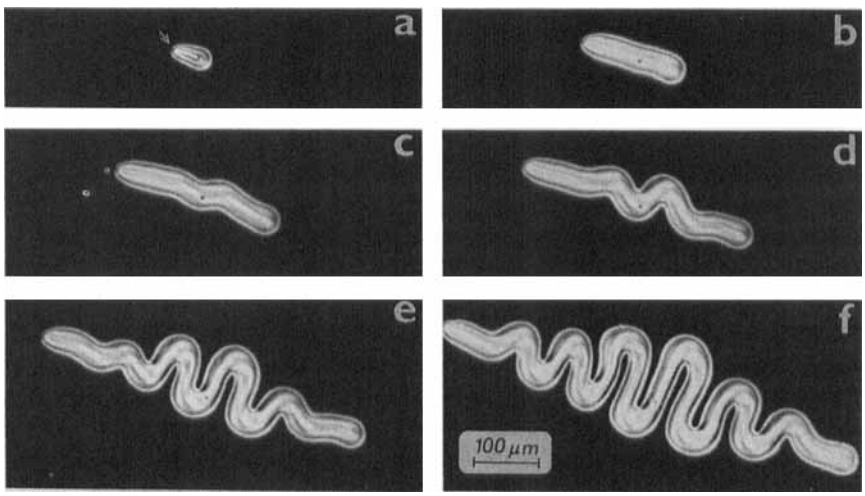

Figure 4. Growth of an isolated finger near the critical line V_2 ($C = 1{\cdot}52$, $V = 4{\cdot}5$ V, $f = 100$ Hz): (*a*) $t = 0$ s, (*b*) $t = 10$ s, (*c*) $t = 20$ s, (*d*) $t = 30$ s, (*e*) $t = 45$ s, (*f*) $t = 60$ s. The arrow indicates an abnormal tip.

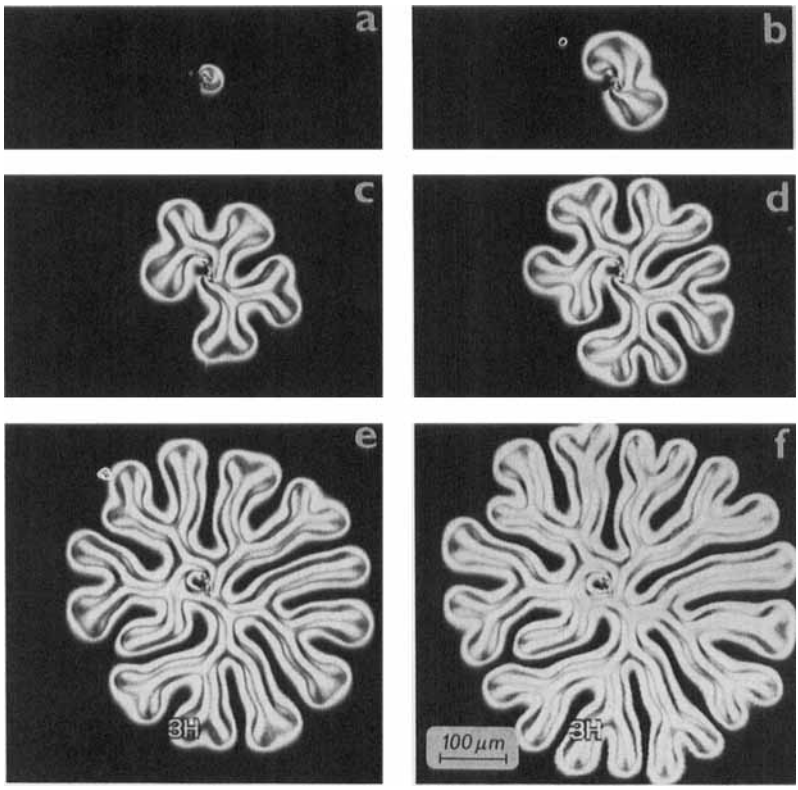

Figure 5. Growth of a periodic pattern of splitting fingers near the line V_0 ($C = 1{\cdot}0$, $V = 2{\cdot}5$ V, $f = 30$ kHz): (*a*) $t = 0$ s, (*b*) $t = 15$ s, (*c*) $t = 30$ s, (*d*) $t = 40$ s, (*e*) $t = 60$ s, (*f*) $t = 70$ s.

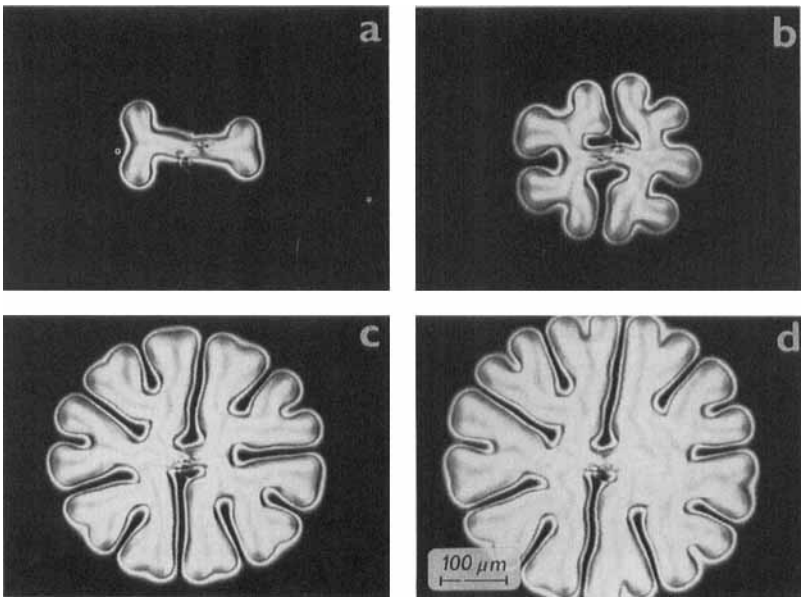

Figure 6. Shape of a periodic pattern at different voltages ($C = 1{\cdot}29$, $f = 100$ Hz) 20 s after switching on voltage: (*a*) $V = 2{\cdot}5$ V, (*b*) $V = 2{\cdot}0$ V, (*c*) $V = 1{\cdot}0$ V, (*d*) $V = 0$ V.

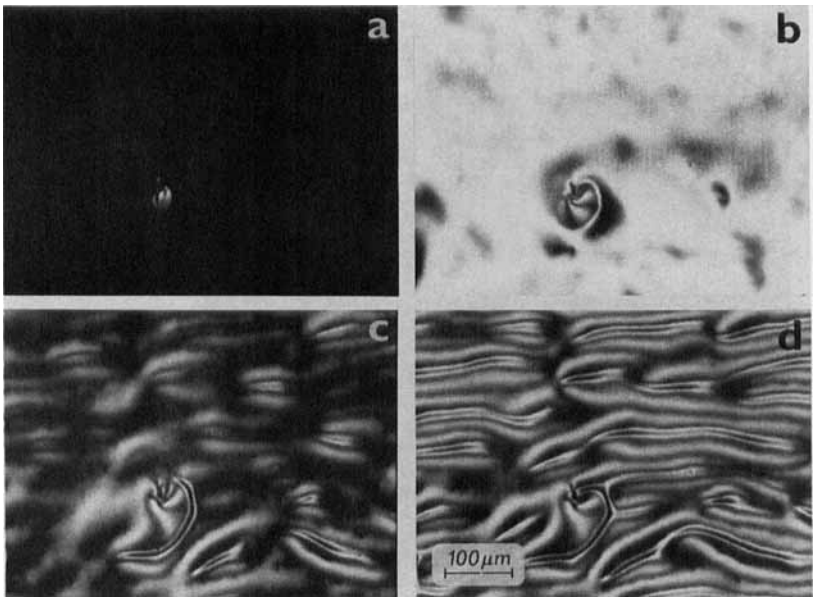

Figure 7. Spontaneous and homogeneous development of the TIC and of a subsequent periodic texture after switching the voltage from 0 V to 13 V ($f = 5$ kHz, $C = 0{\cdot}94$): (*a*) $t = 0$ s, (*b*) $t = 1$ s (TIC), (*c*) $t = 10$ s, (*d*) $t = 18$ s.

(7) The fingers undulate spontaneously as soon as their length exceeds some critical value (see figure 4), especially near the region *D*. This undulation results from a balance between the energy decrease due to a larger area of finger and the elastic energy increase due to its local bending [1].

(8) A simultaneous development of the fingers (nucleating on dust particles) and the TIC can be observed at voltage values near the line V_0.

If the d/p ratio is lower than approximately 0·55, no periodic patterns appear and V_0 corresponds to the Fréedericks transition (see figure 11). Nevertheless, the planar texture is slightly optically active at a higher voltage. Unfortunately, the boundary between regions *F* and *E* was somewhat vague from the experimental viewpoint.

The line V_2 represents the critical line along which the nematic and the cholesteric phase coexist. V_3 and V_0 are the spinodal limits of both phases, while V_{00} characterizes the finger–TIC transition. Finally, V_1 delineates the two regions of different finger growth mode, i.e. isolated growth with stable ends and a periodic pattern formation with ends susceptible to splitting.

In agreement with Lequeux [8] and Ribiere [2], for a thickness d exceeding approximately $0{\cdot}7 \times p$, the phase transition is of the first order, whereas for smaller values, the transition is of the second order. Thus, the Landau tricritical point exists at the intersection of $V_i(C)$ lines (except V_{00}). In the triple point, V_0 and V_{00} lines meet and the nematic phase, the modulated texture, and the TIC coexist at this point. Below C_{tc}, the regularity of the striped textures decreases with decreasing C and are absent for d/p ratios occurring under the triple point. Unfortunately, due to the very gradual decrease in the regularity, the V_{00} value determination was impossible in the vicinity of the triple point. Approximately, C_t acquires a value in the interval from 0·45 to 0·6.

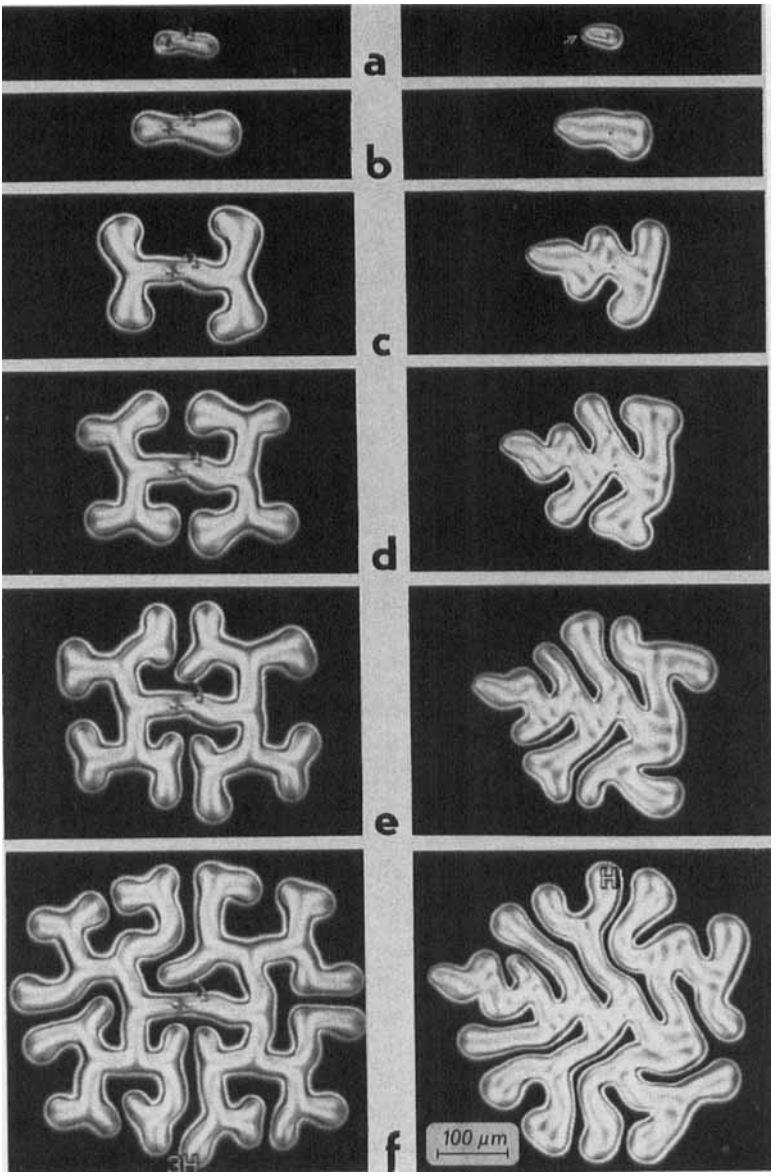

(A) (B)

Figure 8. (A) Growth and splitting of a finger with both tips normal ($C=1{\cdot}29$, $V=2{\cdot}5$ V, $f=100$ Hz): (*a*) $t=0$ s, (*b*) $t=10$ s, (*c*) $t=30$ s, (*d*) $t=40$ s, (*e*) $t=50$ s, (*f*) $t=70$ s. (B) Growth and splitting of a finger with two different tips ($C=1{\cdot}52$, $V=4$ V, $f=0$ Hz): (*a*) $t=0$ s, (*b*) $t=7$ s, (*c*) $t=14$ s, (*d*) $t=21$ s, (*e*) $t=28$ s, (*f*) $t=40$ s. The arrow indicates an abnormal tip.

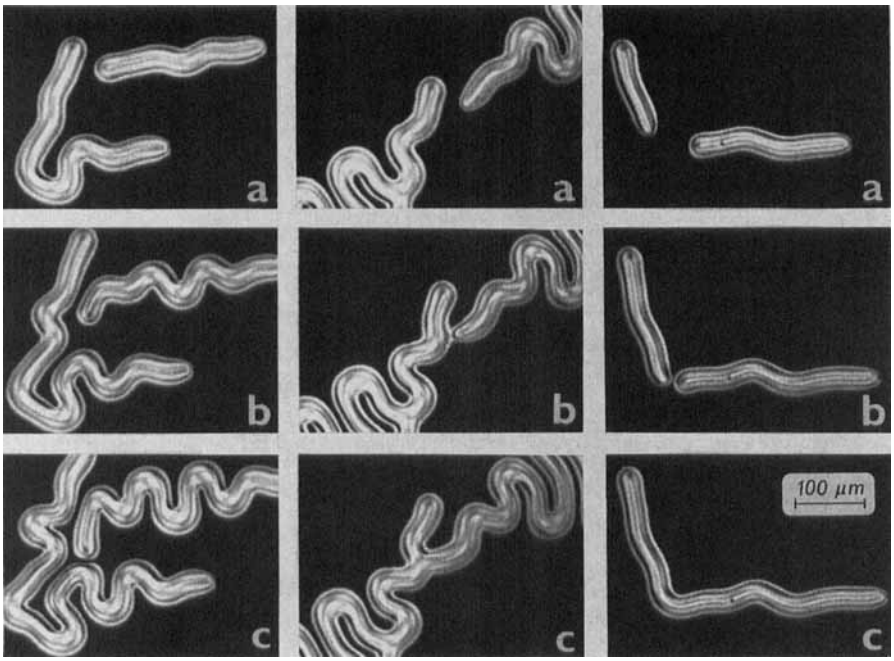

(A) (B) (C)

Figure 9. (A) Growth of a normal tip in the neighbourhood of another finger ($C=1{\cdot}65$, $V=5\,\text{V}$, $f=100\,\text{Hz}$): (*a*) $t=0\,\text{s}$, (*b*) $t=8\,\text{s}$, (*c*) $t=16\,\text{s}$. (B) Junction of an abnormal finger tip with the side of another finger ($C=1{\cdot}65$, $V=5\,\text{V}$, $f=100\,\text{Hz}$): (*a*) $t=0\,\text{s}$, (*b*) $t=5\,\text{s}$, (*c*) $t=8\,\text{s}$. (C) Fusion of an abnormal finger tip with a normal one ($C=1{\cdot}42$, $V=4{\cdot}7\,\text{V}$, $f=100\,\text{Hz}$): (*a*) $t=0\,\text{s}$, (*b*) $t=16\,\text{s}$, (*c*) $t=19\,\text{s}$.

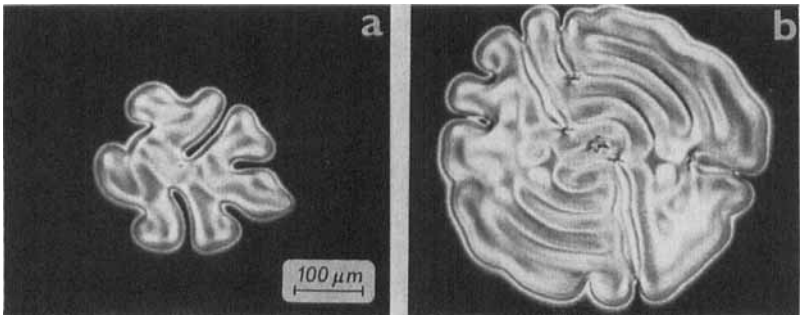

Figure 10. Shape of a periodic pattern at different d/p ratios 60 s after switching on the voltage ($V=3{\cdot}5\,\text{V}$, $f=15\,\text{kHz}$): (*a*) $C=1{\cdot}52$, (*b*) $C=1{\cdot}78$.

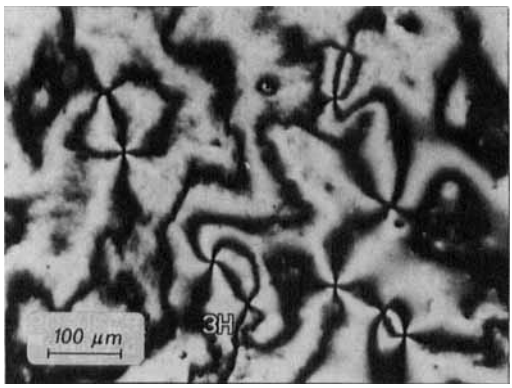

Figure 11. Texture arising after switching on the voltage in a case that the transition is of second order ($C = 0{\cdot}48$, $V = 5$ V, $f = 30$ kHz).

General properties of both the experimental phase diagrams can be explained based on the generalizations of the Ribiere and Oswald theoretical model [1] with two order parameters [2]. However, lack of knowledge of the elastic constants for the mixture investigated prevents the calculation of the phase diagram.

This work has been supported by the Laboratoire de Physique at the École Normale Superieure de Lyon.

References

[1] RIBIERE, P., and OSWALD, P., 1990, *J. Phys., France*, **51,** 1703.
[2] RIBIERE, P., PIRKL, S., and OSWALD, P., 1991, *Phys. Rev.* A, **44,** 8198.
[3] RIBIERE, P., PIRKL, S., and OSWALD, P., 1992, *Presented at the 14th International Liquid Crystal Conference*, Pisa, Italy, B–P29.
[4] BREHM, M., FINKELMANN, H., and STEGEMEYER, H., 1974, *Ber. Bunsenges. phys. Chem.*, **78,** 883.
[5] HARVEY, T. B., 1978, *Molec. Crystals liq. Crystals Lett.*, **34,** 224.
[6] PIRKL, S., 1991, *Cryst. Res. Technol.*, **26,** 371.
[7] PIRKL, S., 1991, *Cryst. Res. Technol.*, **26,** K111.
[8] LEQUEUX, F., OSWALD, P., and BECHHOEFER, J., 1989, *Phys. Rev.* A, **40,** 3974.